Journal of Applied Polymer Science

Lauric Acid Coated Fly Ash as a Reinforcement in Recycled Polymer Matrix Composites

Shubhalakshmi Sengupta,[1] Dipa Ray,[1] Aniruddha Mukhopadhyay,[2] Suparna Sengupta,[3] Tanusree Kar[4]

[1]Department of Polymer Science and Technology, University of Calcutta, 92, Acharya Prafulla Chandra Road, Kolkata 700009, India
[2]Department of Environmental Science, University of Calcutta, 35, Ballygunge Circular Road, Kolkata 700019, India
[3]Calcutta Institute of Engineering and Management, Tollygunge, Kolkata 700040, India
[4]Department of Materials Science, Indian Association for the Cultivation of Science, 2A and B, Raja Subodh Chandra Mallick Road, Kolkata 700032, India
Correspondence to: D. Ray (E-mail: roy.dipa@gmail.com)

ABSTRACT: Sustainable composites were developed from fly ash (FA) and recycled polypropylene (R) with lauric acid (LA) as the coupling agent. The FA particles were surface-coated with 1, 2, 3, and 5 wt % LA, and the coating on the FA particles was verified by transmission electron microscopy and Fourier transform infrared spectroscopy. R and LA-coated FA particles were melt-mixed in a 1:1 weight ratio to achieve a high-filler-loaded composite. The flexural, impact, nanoindentation, and fracture surface analyses were carried out to examine the properties of the composites. The flexural strength and modulus values increased in the 2 wt % LA-coated FA/R composites by 6 and 50%, respectively, compared to the values of the uncoated FA/R composites, whereas the impact strength increased considerably by 119% in the 1 wt % LA-coated composites. Nanoindentation tests also showed an increase in the mechanical properties in the case of the 1 and 2 wt % LA-coated composites in comparison to the uncoated ones. Fracture surface studies done by scanning electron microscopy revealed improved interfacial interactions between the filler and matrix in the presence of the LA coupling agent. X-ray diffraction (XRD) studies indicated reorientations of the polymer chains in the presence of different concentrations of the LA coupling agent; this resulted into different crystallinities and crystallite sizes. Differential scanning calorimetry showed a significant difference in the crystalline peaks of the composites, and this corroborated well with the XRD observations. LA, thus, significantly influenced the structural properties of the composites, and this, in turn, influenced their mechanical and thermal properties. © 2014 Wiley Periodicals, Inc. J. Appl. Polym. Sci. **2015**, *132*, 41586.

KEYWORDS: composites; glass transition; mechanical properties; recycling

Received 25 June 2014; accepted 1 October 2014
DOI: 10.1002/app.41586

INTRODUCTION

The development of value-added sustainable composite materials is an utmost necessity in today's world.[1] Thus, the use of a hazardous industrial waste such as fly ash (FA) and a consumer waste such as recycled polypropylene (R) to develop value-added novel materials is an interesting approach.[1,2] FA, a waste generated from thermal power plants, varies in composition depending on the source of coal. It is composed primarily of SiO_2 along with lower contents of Al_2O_3, Fe_2O_3, Na_2O, MgO, and K_2O.[3,4] Several researchers have investigated innovative ways of establishing FA as a mineral filler in polymer matrix composites having different engineering applications;[3,5–7] this would enable their removal from the environment and recycle them through the development of composites having application potential.

Ramakrishna et al.[8] observed improvements in the tensile and flexural strengths in 40% FA-filled 4% poly(methyl methacrylate)-toughened epoxy matrix composites. Gupta et al.[9] reported an increase in the impact properties on the addition of FA in glass fiber/epoxy composites. Menon et al.[10] investigated the use of FA as a filler in natural rubber in the presence of 5–10 phr phosphorylated cardanol prepolymer and a hexamethylenetetramine-cured phosphorylated cardanol prepolymer. This resulted in a higher thermal stability along with an improvement in the mechanical properties. Sridhar et al.[6] reported an increase in the thermal stability in FA/waste tire powder/isotactic polypropylene (PP) composites with increasing FA content. Ray et al.[4] studied changes in the mechanical properties of vinyl ester resin matrix composites that contained 30, 40, 50, and 60 wt % FA filler. They reported that FA could be used effectively to increase the rigidity and stiffness of the

vinyl ester resin matrix; however, there was a decrease in the properties above a 50 wt % FA loading. In a separate study, these composites showed faster thermal degradation at a lower temperature, particularly in the 30 and 60 wt % FA-filled composites, and a higher onset temperature for the 40 and 50 wt % FA-filled composites with respect to the vinyl ester matrix.[11]

According to Yu-Fen et al.,[12] an improvement in the composite strength with FA as a filler shows problems with regard to the weak interfacial bonding between the untreated FA and the polymer. So, the modification of FA is done by various techniques where either coupling agents or surfactants have been added to modify the surface characteristics of the FA filler to improve the interfacial bonding with the matrix.[12] Bose and Mahanwar[13] and Nath et al.[14] reported that coupling agents such as titanate and surfactants such as sodium lauryl sulfate (SLS) enhanced the filler/matrix physical bonding with an improvement in the mechanical properties in FA-filled Nylon 6 and poly vinyl alcohol (PVA) composites, respectively. Patil et al.[15] studied the incorporation of nanostructured FAs modified with the surfactant SLS in an ethylene–octene copolymer. Surface modification resulted in better interfacial adhesion between the modified FA and the polymer and led to improved mechanical properties. Bonda et al.[16] reported that the surface treatment of FA particles by bis(3 triethoxysilylpropyl) tetrasulfane (Si69) improved the interfacial adhesion between the acrylonitrile–butadiene–styrene and FA and resulted in an improvement in their mechanical properties. The use of a titanate coupling agent (LICA 38) at different weight percentages in the FA–PP composites improved the interfacial interaction between the filler and the matrix, and an enhancement in the mechanical and thermal properties of the composites occurred.[17] Pardo et al.[3] reported improved stiffness, strength, and thermal stability in FA/isotactic PP composites where silane coupling agents containing three different reactive functional groups, amine (GF96), vinyl (XL10), and vinyl benzyl amine (Z-6032), were used. The vinyl- and aminosilane-treated FAs showed better results because of strong filler–matrix adhesion.

Das et al.[18] reported the use of R through the formation of composites with a 50 wt % loading of FA with vinyl trimethoxyl silane (VTMO) and maleated PP (Epolene G3003) coupling agents. The mechanical properties and thermal stability were found to be much higher in the VTMO-treated composites compared to the untreated ones because of enhanced interaction at the filler–matrix interface in the presence of VTMO.[18] Stearic acid (SA) has been used as a surface modifier for fillers such as nano-alumina in ethylene propylene diene monomer (EPDM) composites, for a calcium carbonate nanoparticle coating in a PP matrix, and for the surface coating of FAs in PP/ethylene vinyl acetate/high density polyethylene composites.[19–21]

In our earlier studies, SA, palmitic acid (PA), and furfuryl palmitate (FP) were used for to surface-coat FA particles, which were subsequently used as reinforcements in R matrix composites. These fatty acids, having carbon chain lengths of 16 (PA, FP) and 18 (SA) were observed to have considerable influence on the filler/matrix interface and to have reoriented the crystalline arrangement of the polymer chains and modified the structural properties of the composites. The use of 1–2 wt % of these fatty acids as a coupling agent in FA/R composites showed improvements in the mechanical and thermal properties.[22–25]

In this study, which was a continuation of our previous work, lauric acid (LA), a medium-chain-length (12-carbon) fatty acid was used for the first time as a coupling agent in an FA/R composite. The efficacy of this nonconventional green coupling agent in the FA/R composite, where the filler and matrix were present in equal proportions, was investigated in this study. The evaluation of the mechanical and structural properties of the composite samples and the analyses of the surface coating and the interfacial interaction between the surface-coated FA particles and the polymer matrix were carried out.

EXPERIMENTAL

Materials

FA used was collected from Kolaghat Thermal Power Station (India). This ASTM class F FA (as per ASTM C 618) was found to have different proportions of oxides (59% SiO_2, 21% Al_2O_3, 8% Fe_2O_3, and other oxides).[11] The ash particles had the following particle size distribution: 10% had a particle size below 2.38 μm, 50% had a particle size below 13.58 μm, and 90% had a particle size below 111.16 μm. R was obtained from recycled postconsumer plastic products and was used as the matrix material. LA and acetone were obtained from Loba Chemie Pvt., Ltd. (Mumbai, India).

Surface Treatment of the FA and the Fabrication of the Composites

LA was dissolved in a blend of acetone and toluene. FA particles were immersed in this solution followed by stirring for 15 min. Four separate sets of coated FA particles were prepared with 1, 2, 3, and 5 wt % LA, respectively. The surface-coated FA particles were designated as FALAX, where *X* denotes the weight percentage of LA with respect to the weight of coated FA. The surface-coated FA particles and the R were melt-mixed in a 1:1 weight ratio in an internal melt mixer (Brabender 30/50 E, Germany) at a temperature of 170°C. A similar set was also prepared with uncoated FA particles and R. The resulting melt-mixed compounds were compression-molded at 170°C to form the composite sheets. The composites were designated as RFALA0, RFALA1, RFALA2, RFALA3, and RFALA5, and the unreinforced composite was designated as R.

Characterization of the FA Particles

Transmission Electron Microscopy (TEM). TEM (JEM 2100 HR, JEOL, Japan) with energy-dispersive X-ray spectroscopy (EDS) was used with a field emission gun; this provided high-resolution operation at 200 kV and 1.05 μA. The FA particles, both coated (FALA1 and FALA5) and uncoated (FA), were dispersed in ethanol and then sonicated. A drop of the diluted suspension was poured onto a copper grid and air-dried. The EDS quantitation method was the Cliff Lorimer thin-ratio section.

Fourier Transform Infrared (FTIR) Spectroscopy. IR spectra of the FA particles were obtained with a PerkinElmer IR spectrometer (Spectrum RX 73713 series). We prepared the samples by making KBr pellets containing powders of approximately 0.75 wt %.

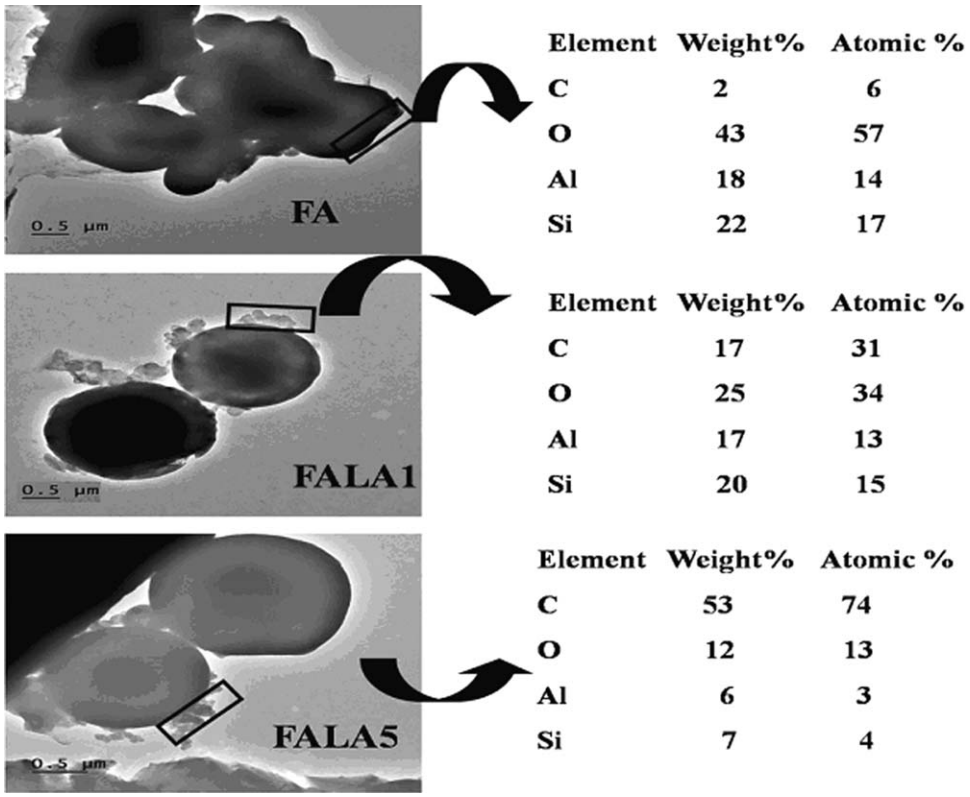

Figure 1. TEM analyses of FA, FALA1, and FALA5 particles and the EDS data of the FA surfaces.

Characterization of the Composites. ***Flexural and impact testing.*** The composite samples were tested for their flexural properties under three-point bending in an Instron 4303 instrument (Norwood, MA) in accordance with ASTM D 790-10. Five samples of each set were tested to obtain the mean value, and the standard deviation is also reported. The flexural strength and flexural modulus values were studied up to 5% strain for R.[26] The impact strengths of the samples were tested in a CEAST Izod impact tester (WinPEN CEAST S. p. A, Turin, Italy) according to ASTM D 256-10. Five samples of each set were tested to obtain the mean value, and the standard deviation was calculated. The statistical analysis was done with Origin 8 software (Origin Lab Corp., Northampton, MA), and all the graphs in this study were plotted with this software. The test values were also statistically analyzed (paired *t* test) between the uncoated FA/R (RFALA0) composites and the LA-coated FA/R composites (RFALA1, RFALA2, RFALA3, and RFALA5, respectively) to determine whether the differences incurred were statistically significant through the use of Minitab 13 software (Minitab, Inc., State College, PA).

Nanoindentation. The nanoindentation studies of the composite samples were carried out with a CSM NHTX S/N: 55-0019 nanohardness tester (CSM, Switzerland) with a triangular pyramidal diamond indenter (Berkovich, B-I 93, radius of curvature = 20 μm) under a constant load of 100 mN under an incremental cyclic loading mode of three successive cycles. The instrumented hardness (H_{IT}), instrumented elastic modulus (E_{IT}), and Vickers hardness number (H_v) were estimated by Oliver and Pharr analysis.[27]

Scanning electron microscopy (SEM). The fracture surface of the composite samples were coated with Au–Pd alloy and investigated under SEM (Hitachi S-3400N, Krefeld, Germany).

X-ray diffraction analysis (XRD). XRD analysis was done with an X-ray diffractometer (X Pert Pro, PANalytical, Almelo, The Netherlands) with Cu Kα radiation operating at 40 kV and 30 mA at a scanning rate of 2°/min in the diffraction angle range of $2\theta = 5$–90°. R and all of the composites were examined.

Differential scanning calorimetry (DSC). DSC analysis of the composite samples (5–10 mg) was carried out with a DSC Q20 V 24.4 Build 116 instrument (TA Instruments, New Castle, DE) at a heating rate of 10°C/min in the temperature range between −50 and 200°C in a nitrogen environment. The cooling and second heating were then done at the same rate to evaluate the thermal-transition behavior of the composites.

RESULTS AND DISCUSSION

Analysis of the FA Particles

The coated and uncoated FA particles were examined with TEM and FTIR spectroscopy. The data for FA, FALA1, and FALA5 are given here.

TEM

The TEM images of FA, FALA1, and FALA5 are shown in Figure 1. A greater agglomeration effect was evident with the uncoated FA particles; this seemed to decrease in FALA1 and FALA5 with the surface coating. This type of phenomenon was witnessed earlier in SLS-coated FA particles, where the surface coating of FAs reduced the interfacial interactions between the

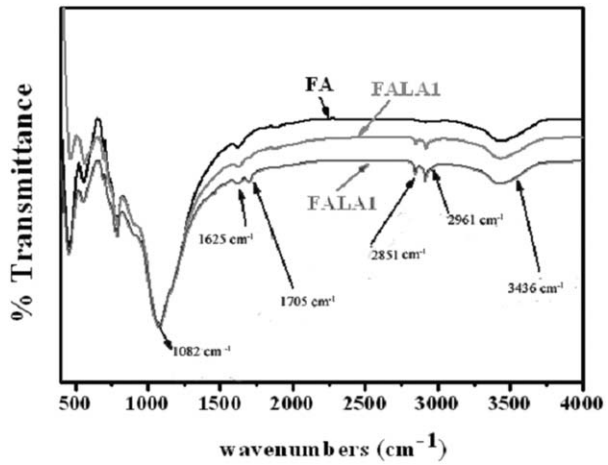

Figure 2. FTIR spectra of FA, FALA1, and FALA5.

unmodified particles and led to a reduction in the agglomeration of the particles in the composites.[14] In FALA1 and FALA5, clusters of particles were seen on the surface; this could have been due to the presence of fatty acid. The EDS spectra of those regions on the surface of the FAs were analyzed, and a high percentage of carbon content was present (53 wt % in FALA5) with respect to the regions in FA having no agglomerates (Figure 1). This indicated that those regions were rich in carbon because of the presence of fatty acids. In an earlier study, an increase in the amount of carbon content on the carbonaceous agglomerate present on the FA surfaces was witnessed for SLS-surface-modified coal FAs.[28] Thus, visually, the surface coating of the FA particles was witnessed. The chemical evaluation of the surface-coated FA particles was further carried out through FTIR spectroscopy.

FTIR Spectroscopy

The FTIR spectra of FA, FALA1, and FALA5 are shown in Figure 2. The stretching bands of Si—O—Al bands mainly appeared in the range 1200–600 cm^{-1} for the vibrations of the Si—O and Al—O bands in FA.[14] The broad band at 1082 cm^{-1} was attributed to Si—O stretching, and the absorption bands at 1625 and 3436 cm^{-1} were attributed to the —OH absorption bands.[21,29] In surface-coated FA particles, especially in FALA5, the bands at 2851 and 2918 cm^{-1} were related to C—H band symmetric stretching vibrations and asymmetric stretching vibrations, respectively; this helped us to identify $—CH_2$ group of the fatty acid. The $—CH_3$ group was also visualized by a small asymmetric stretching vibration of —C—H bond, which occurred at 2961 cm^{-1}. These observations proved the presence of LA on the FA surface. Similar FTIR absorption peaks of SA-coated coal FA were reported earlier.[21] The carboxylate peak —C═O at 1705 cm^{-1} [30] also indicated the presence of the fatty acid. Thus, from earlier reports,[2,21] our previous studies,[22] and our present observations, we inferred that the surface coating of the FA particles by LA occurred as a result of physical interactions between the metal—OH groups of FA and the polar part of the fatty acid with the nonpolar part available for compatibilization with the polymer chains. These FA particles were incorporated into composites in high proportion (50 wt %), and the efficacy of LA as a coupling agent was studied. FTIR analysis of the uncoated FA-filled R (RFALA0) and RFALA5 (having the highest weight percentage of LA) are given in the Supporting Information (Figure S1). The plots reveal the characteristic peaks of FA and those corresponding to PP.

Flexural and Impact Testing

The variations of the flexural strength and modulus of the unreinforced R and the composites (RFALA0, RFALA1, RFALA2, RFALA3 and RFALA5) are given in Figure 3. We observed that the flexural strength decreased with the addition of FA by 68% in RFALA0 in comparison to that of R. A decrease in the flexural strength on the incorporation of filler in vinyl ester resin matrix composites in the presence of organoclay was reported earlier.[31] The incorporation of filler by 50 wt % in the R matrix reduced the polymer chain entanglements as FA particles entered between the R chains. Among the coated composites, the flexural strength increased in RFALA2 by 6% but decreased by 22, 3, and 20% in RFALA1, RFALA3, and RFALA5, respectively, in comparison to that observed in RFALA0. This increase in the flexural strength was attributed to the enhancement in the stress transfer at the interface between the 2 wt % LA-coated FA particles and the polymer matrix. The decreases in the flexural strength in RFALA1, RFALA3, and RFALA5 were attributed to the reduced mechanical interlocking between the R chains and FA as a result of the smoothening of the FA particle surface; this did not provide the mechanical anchorage provided by the rough surface of the uncoated FA particles to the polymer chains.[22] Two opposite phenomenon were operative at the interface: mechanical anchorage of the polymer chains onto the filler surface, which was more pronounced in the uncoated FA particles, and filler/matrix compatibilization at the interface through the fatty acid coupling agent, which was more predominant with the coated FA particles. Preferential dominance of one factor over the other controlled the stress transfer at the interface.

The modulus values of RFALA0 increased by 67% from that of R. The incorporation of the filler increased the flexural modulus

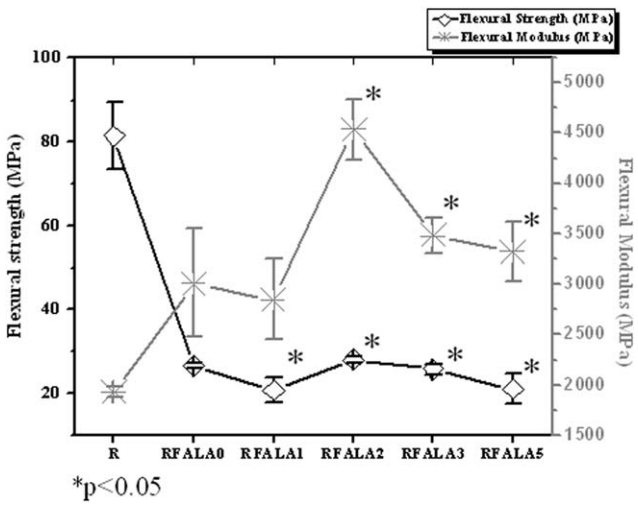

Figure 3. Flexural strength and flexural modulus values of R and the composite samples. (The values marked with an asterisk are statistically significant.)

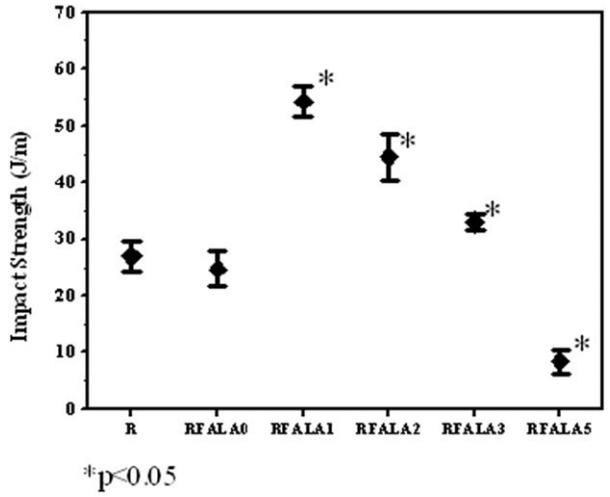

Figure 4. Impact strengths of R and the composite samples. (The values marked with an asterisk are statistically significant.)

of the composite because of the restriction in chain mobility, and such an increase in the flexural modulus with decreasing flexural strength in PP on the incorporation of a filler was reported in a previous study.[22] The modulus values increased by 50, 16, and 10% in RFALA2, RFALA3, and RFALA5, respectively, and decreased by 6% in RFALA1, respectively, compared to that of RFALA0. This implied that at 1 wt % LA, physical entanglement of the filler with the matrix was not adequate to achieve enhanced modulus values. A similar observation was reported earlier.[23] Thus, RFALA2 showed the highest enhancement in both flexural strength and modulus among the composites.

As discussed earlier, the presence of the coupling agent influenced the interfacial bonding and the mechanical properties of the composites. The use of the conventional silane coupling agent in the FA/R matrix was studied earlier, where it was reported that a 6 wt % Dynasylan VTMO-treated composite showed increases of 4 and 15% in the flexural strength and modulus, respectively, in comparison with the untreated ones.[18] When compared with silane coupling agents, these long-chain fatty acids, that is, stearic, palmitic, and ester FP, LA has been found to render efficient coupling action at a lower percentage that is, at 2 wt %. LA (RFALA2) showed the highest enhancement in the flexural modulus values (4535 MPa) when compared to our previous reports, where 1 wt % SA- and PA-coated FA/R and 2 wt % FP-coated FA/R composites showed flexural modulus values of 4294, 4522, and 3054 MPa, respectively.[22–24]

The impact strengths of R and the composites were also studied (Figure 4). The impact strength decreased in RFALA0 (25 J/m) from that of R (27 J/m). The impact strengths increased by 119, 80, and 33% for RFALA1, RFALA2, and RFALA3, respectively, compared to that of RFALA0 and decreased by 66% in RFALA5. Thus, LA aided in enhancing the impact strength of the composites. This observation indicated that the alignment of the R molecules in the presence of LA at the interface led to different crystalline arrangements, and the impact strength was influenced accordingly. In comparison with our earlier studies, LA proved to be as efficient as the other fatty acids; it had almost the highest enhancement of impact strength in RFALA1 (54 J/m), which was second only to RFAPA1 (57 J/m).[23]

Nanoindentation

Nanoindentation was carried out to evaluate the micromechanical properties and hardness values of the composites. Table I shows the variation of the elastic modulus [Young's modulus calculated from the load-displacement plot of the instrumented nanoindentation test (E_{IT})] and hardness (H_{IT} and H_v) of the samples where the penetration of the indent took place at a constant load of 100 mN. The penetration of the indenter in the polymer matrix was due to the mobility of the polymer chains.[32] On incorporation of the filler, this mobility of the polymer chains was restricted; this resulted in increased stiffness and higher resistance to the indenter along with an enhanced hardness value, as was witnessed in RFALA0, where H_{IT}, E_{IT}, and H_v increased by 7, 32, and 9%, respectively, compared with those of R. The enhancement in the hardness values on the addition of FA as a filler in polymer composites was also reported earlier.[33] In the presence of the coupling agent, the hardness values (H_{IT} and H_v) increased by 4 and 2% in RFALA1, respectively, and 4 and 2% in RFALA2, respectively, when compared to those of RFALA0. In the case of RFALA3 H_{IT} increased nominally by 1%, and there was no increase in the H_v value compared to that of RFALA0. In RFALA5, H_{IT} and H_v decreased by 5 and 8%, respectively. Therefore, the presence of 3 and 5 wt % LA at the FA/R interface did not significantly improve the hardness values (H_{IT} and H_v). The E_{IT} values increased by 3% in RFALA2 but decreased by 9, 6, and 12% in RFALA1, RFALA3 and RFALA5, respectively, when compared that of to RFALA0. Therefore, the stiffness of the material measured on its surface at the point of contact with the indentation tip revealed that presence 2 wt % LA in the FA/R composite increased its mechanical strength.

Thus, a significant improvement in the mechanical properties was witnessed in the presence of LA; this was a result of better interfacial interaction between the filler and the matrix.

SEM

To clearly visualize the filler–matrix interactions, the fracture surfaces of the composites were investigated under SEM (Figure 5). In RFALA0, the adhesion of the FA particles with the matrix was poor when compared with the rest of the composite samples. In the composites where surface-coated FA particles were present, improved interfacial bonding was evident, with most significant in the cases of RFALA1 and RFALA2. In the cases of

Table I. Nanoindentation Values of R and the Composite Samples

	H_{IT} (MPa)	E_{IT} (MPa)	H_v
R	445	4290	45
RFALA0	478	5731	49
RFALA1	496	5362	50
RFALA2	495	5873	50
RFALA3	482	5408	49
RFALA5	449	5037	45

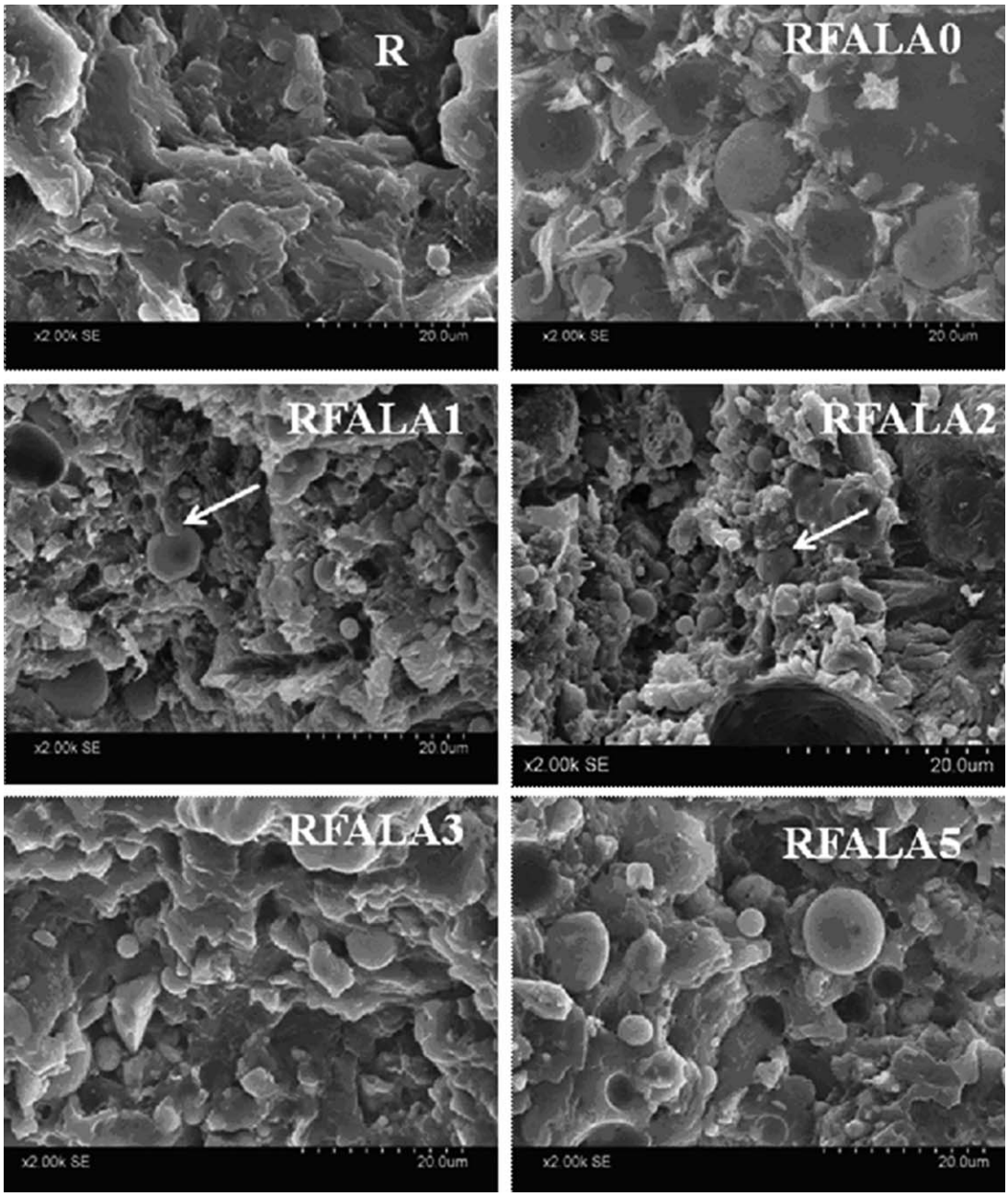

Figure 5. SEM micrograph of the flexural fracture surfaces of R and the composite samples showing filler–matrix interactions.

RFALA1 and RFALA2, the FA particles were uniformly dispersed and encapsulated within the PP matrix (Figure 5) and showed good interfacial interaction. However, in the cases of RFALA3 and RFALA5, larger agglomerates were visible; these might have been responsible for the reduction of the mechanical properties. Higher concentrations of LA (3 and 5 wt %) at the interface thus caused an agglomeration effect, whereas 1 and 2 wt % LA were found to be the optimum concentrations. To further evaluate the influence of the structural reorganization on the mechanical properties in the presence of LA, XRD and DSC analyses were carried out.

XRD Analysis

The crystalline morphology of the matrix was influenced considerably by the presence of LA moieties at the interface; this was investigated by XRD analysis. The percentage crystallinity and crystallite size values of the unreinforced R and R in the composites were calculated from the XRD data with Scherer's equation:

$$L_{h,k,l}=K\lambda/\beta \cos \theta \quad (1)$$

where $L_{h,k,l}$ is the crystallite size of the crystalline plane, λ is the X-ray wavelength, K is the shape factor ($K = 0.94$), β is the full-

Table II. Percentage Crystallinity (%C) and Crystallite Size (CS) of R and the Composite Samples Obtained from the XRD Analysis

		Peak position (2θ)				
Sample	Parameter	14	17	18	21	22
R	%C	80	95	65	65	68
	CS	52	47	52	47	37
RFALA0	%C	80	81	—	84	—
	CS	21	21	—	11	—
RFALA1	%C	88	69	72	59	82
	CS	86	52	85	86	73
RFALA2	%C	88	89	73	63	73
	CS	64	86	43	125	64
RFALA3	%C	64	88	84	58	72
	CS	156	72	86	43	129
RFALA5	%C	72	61	84	83	61
	CS	129	64	65	85	43

width at half-maximum perpendicular to each plane, and θ is Bragg's angle.[22] The percentage crystallinity was calculated per the following formula for each crystalline plane of the matrix:[22]

$$\text{Crystallinity } (\%) = \left(I_{h,k,l} - I_{\text{amp}}\right)/I_{h,k,l} \times 100 \qquad (2)$$

where $I_{h,k,l}$ corresponds to the maximum intensity of the particular α monoclinic planes of either (110), (040), (130), (111), or (131), respectively, and I_{amp} corresponds to the intensity of the amorphous region. The calculated percentage crystallinity and crystallite size values are given in Table II. R showed a diffraction pattern similar to a semicrystalline polymer, and R with the incorporation of FA and surface-coated FA showed similar XRD patterns as reported earlier.[22] Among all of the LA-treated composites, the highest increases in percentage crystallinity and crystallite size were observed in the RFALA2 (110) plane, followed by RFALA1. A significant increase in the crystallite size in all of the LA-treated FA/R composites was observed in comparison to our earlier studied FA/R composites with SA and PA coupling agents, as shown in Figure 6.[22,23] This was attributed to the fact that LA was a shorter chained fatty acid with a lower molecular weight than PA and SA had a greater accessibility in the R matrix. The incorporation of FA resulted in a nucleating effect in the R matrix; this resulted in smaller regions of crystallization and a reduction in the crystallite size.[34] This changed in the presence of the coupling agents, as reported earlier.[23] When fatty acids such as SA, PA, or LA are used as coupling agents and the main filler/matrix compatibilization at the interface occurs through the interaction between the hydrocarbon chain of the fatty acid and the R molecules, the fatty acid chain length is likely to play a distinctive role by influencing the crystalline packing of the R molecules. It was reported by Sarazin-Perrin et al.[35] that the presence of a lower molecular weight coupling agent on the filler surface changes the crystallization orientation of the matrix molecules because of its better miscibility in comparison to a higher molecular weight coupling agent, as seen for PP/clay nanocomposites, where coupling agents with different molecular weights (e.g., maleated PP, epolene E43, and polybond 3150) were used. In this study, the presence of a 12-carbon-chain-length fatty acid LA (when compared to our earlier studied 16- and 18-carbon-chain-length PA and SA)[22,23] could render the crystalline reorientation of the polymer matrix; this was different to that of PA and SA. Differences in the molecular structure of the coupling agents renders differences in their interactions with the filler and the matrix. In the presence of LA, smaller crystallites formed because the homogeneous nucleating effect of FA in RFALA0 was not present because of the alterations in the crystalline structure. In its place, larger crystallites were formed.

DSC

The DSC curves of the second heating cycle of R and the composites are shown in Figure 7. The melt crystallization temperature (T_c) and crystallization enthalpy (ΔH_c) obtained from the cooling cycle and the melting point (T_m) and melting enthalpy (ΔH_m) values obtained from the second heating cycle are given in Table III. From the cooling cycle, we observed that the melt crystallization peak temperature during the cooling cycle (T_c) appeared in all of the composites between 113 and 114°C, whereas T_c for the unreinforced R appeared at 123°C. This significant decrease in T_c was due to the presence of 50 wt % filler. The ΔH_c values observed in the cooling cycle of the surface-treated composites were lower than those observed in RFALA0. However, among the composites, RFALA2 showed a slightly higher exothermic ΔH_c value (30 J/g) during melt crystallization compared to the other treated composites.

In the second heating cycle, the R matrix showed a slightly higher single melting peak with higher enthalpy values than the composites. In RFALA0, a single sharp peak (T_m) was observed at 157°C along with a distinct glass-transition temperature at −16°C and a small but distinct endothermic peak at 126°C. A distinct glass-transition temperature was observed in both R and RFALA0 when no coupling agent was present (Figure 7), whereas in all of the LA-coated FA/R composites, no sharp glass transition was observed. This might have been due to the effect of the LA coupling agents at the interface, which restricted the

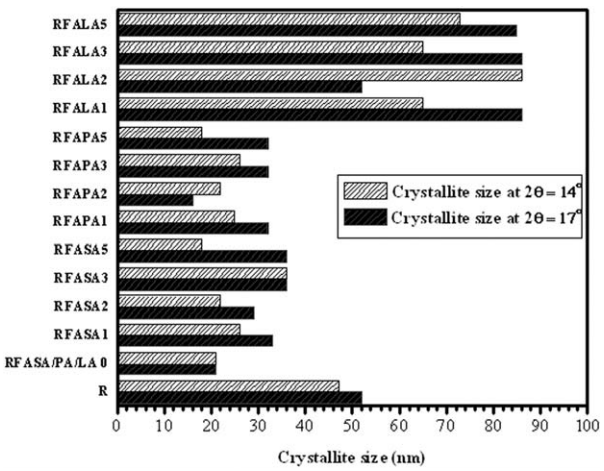

Figure 6. Comparative study of the crystallite sizes of R and the LA-coated composites with those of previously reported values with SA and PA coupling agents[19,20] (at two major peaks $2\theta = 14$ and 17°).

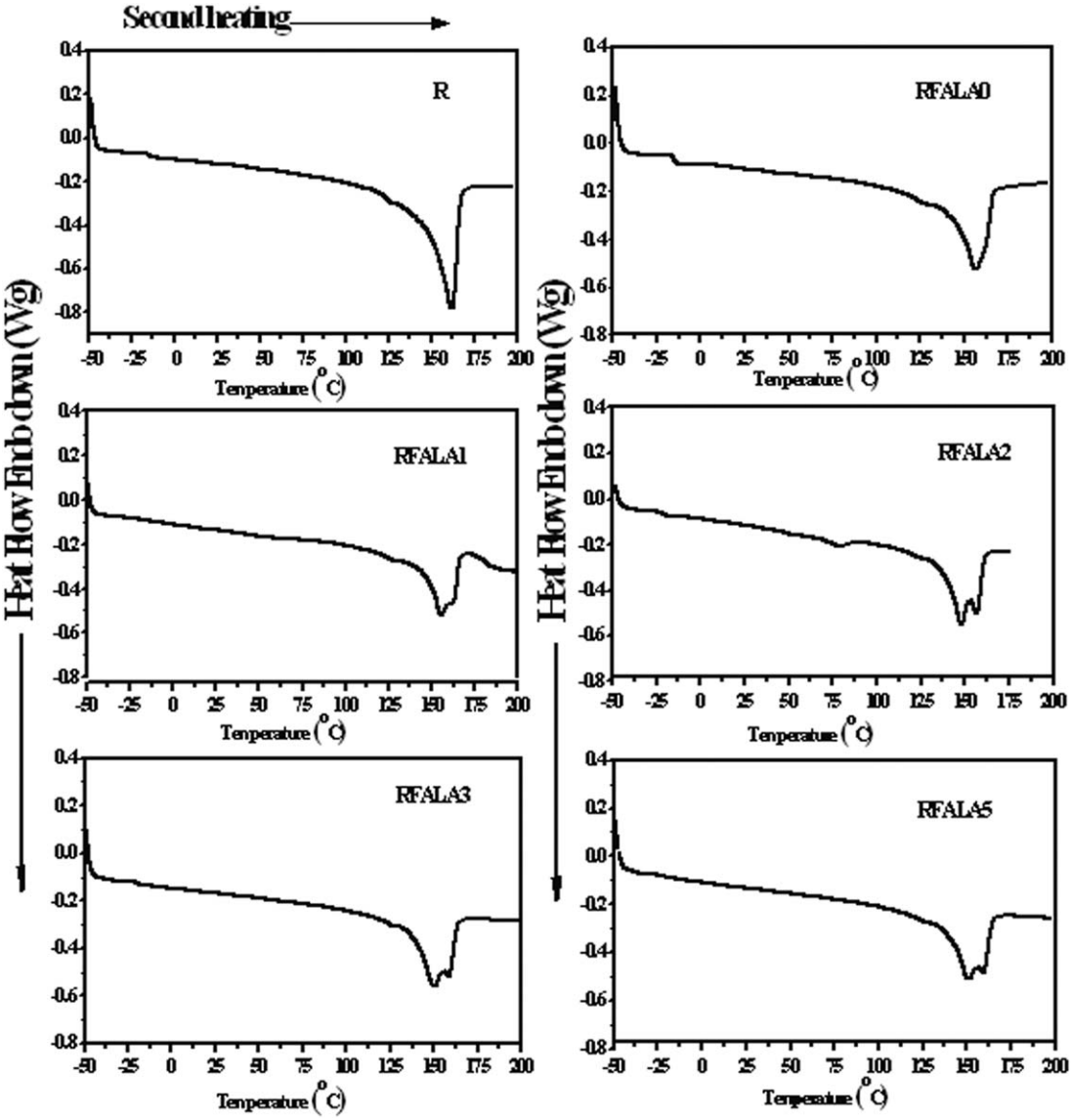

Figure 7. DSC curves (second heating cycle) of R and the composite samples.

chain mobility of the amorphous region of the composites. The presence of multiple peaks in RFALA0 and bimodal melting peaks in the LA-coated FA/R composites could have been related to the occurrence of several crystallographic forms of PP, which were reported earlier.[22] The bimodal peaks also resulted in lower endothermic enthalpy values, with RFALA2 (41 J/g) being the highest among the composites. The high exothermic and endothermic values of RFALA2 among the composites

Table III. T_c, T_m, and Enthalpies of R and the Composite Samples during the DSC Cooling and Second Heating Cycles

	DSC cooling cycle		DSC second heating cycle		
			T_m (°C)		
Sample	T_c (°C)	ΔH_c (J/g)	Major peak	Minor peak	ΔH_m from the major peak (J/g)
R	123	87	162	—	57
RFALA0	113	55	157	—	45
RFALA1	114	39	151	160	26
RFALA2	114	41	147	153	30
RFALA3	113	36	149	155	13
RFALA5	113	35	150	159	

corroborated with the XRD analysis observations, where RFALA2 had the high percentage crystallinity value of 89% at $2\theta = 14°$. Thus, a significant structural reorientation in the R matrix was evident in the presence of the LA coupling agent in the composites.

We concluded from various tests that the enhancement in the mechanical properties, especially in case of RFALA2, was a result of two phenomenon: (1) improved interfacial interaction, especially in the presence of 2 wt % LA, and (2) crystalline reorientation of the R matrix in the presence of LA-coated FA particles. Improvements in the thermal properties were also observed from thermogravimetric analysis (Figure S2, Supporting Information), where the higher onset of degradation was observed in RFALA1 (350°C) followed by RFALA2 (320°C); this indicated a stronger interface and higher crystalline packing of the polymer molecules, which enhanced the thermal stability.

CONCLUSIONS

LA was used for the first time as a coupling agent between R and FA particles, where the filler and matrix were present in a 1:1 weight ratio. The concentration of the coupling agent was varied from 1 to 5% with respect to the FA weight. Efficient surface coating did take place between LA and FA, as evident from the TEM and FTIR studies. This surface coating resulted in an increase in the flexural modulus in RFALA2 with respect to the uncoated FA/R composite because of the enhanced filler–matrix interactions. The impact strength and nanoindentation studies also supported this observation. Crystalline reorientation, along with an increase in the percentage crystallinity, was evident in RFALA2. This structural reorientation was further confirmed by the DSC results. LA was found to be an effective coupling agent for the FA/RPP composites. These composites have the potential to be developed into environmentally friendly and economically sustainable materials that could be used for structural/construction purposes.

ACKNOWLEDGMENTS

One of the authors (D.R.) is thankful to the Department of Science and Technology, Government of India, for granting her the project. Another author (S.S.) is thankful to the Department of Science and Technology for her fellowship. All of the authors are thankful to Himel Chakraborty, School of Material Science and Engineering (SMSE), Indian Institute of Engineering Science and Technology (IIEST), Shibpur, for nanoindentation testing and also to N. R. Bandyopadhyay and Malay Kundu, SMSE, IIEST, Shibpur, for their help in doing the flexural testing of the composite samples.

REFERENCES

1. Parvaiz, M. R.; Mahanawar, P. A.; Mohanty, S.; Nayak, S. K. *Polym. Compos.* **2011**, *32*, 1115.
2. Iraola-Arregui, I.; Potgieter, H.; Liauw, C. M. *Macromol. Mater. Eng.* **2011**, *296*, 810.
3. Pardo, S. G.; Bernat, C.; Abad, M. J.; Caro, J. *Polym. Compos.* **2010**, *31*, 1722.
4. Ray, D.; Bhattacharya, D.; Mohanty, A. K.; Drzal, L,T; Misra, M. *Macromol. Mater. Eng.* **2006**, *291*, 784.
5. Guhanathan, S.; Sarojadevi, M. *Compos. Interface* **2004**, *11*, 43.
6. Sridhar, V.; Xiu, Z. Z.; Xu, D.; Lee, S. H.; Kim, J. K.; Kang, D. J.; Bang, D. *Waste Manage.* **2009**, *29*, 1058.
7. Nath, D. C. D.; Bandyopadhyay, S.; Yu, A.; Blackburn, D.; White, C. *J. Mater. Sci.* **2010**, *45*, 1354.
8. Ramakrishna, H. V.; Padma Priya, S.; Rai, S. K.; Varadarajulu, A. *J. Reinf. Plast. Compos.* **2005**, *24*, 1279.
9. Gupta, N.; Brar, B. S.; Woldesenbet, E. *Bull. Mater. Sci.* **2001**, *24*, 219.
10. Menon, A. R. R.; Sonia, T. A.; Sudha, J. D. *J. Appl. Polym. Sci.* **2006**, *102*, 4801.
11. Ray, D.; Banerjee, S.; Mohanty, A. K.; Misra, M. *Polym. Compos.* **2008**, *29*, 58.
12. Yu-Fen, Y.; Guo-Shen, G.; Zhen-Fang, C.; Qing-Ru, C. *J. Hazard. Mater.* **2006**, *B133*, 276.
13. Bose, S.; Mahanwar, P. A. *J. Appl. Polym. Sci.* **2006**, *99*, 266.
14. Nath, D. C. D.; Bandyopadhyay, S.; Gupta, S.; Yu, A.; Blackburn, D.; White, C. *Appl. Surf. Sci.* **2010**, *256*, 2759.
15. Patil, A. G.; Mahendran, A.; Anandhan, S. *Silicon* **2014**. DOI: 10.1007/s12633-014-9194-2.
16. Bonda, S.; Mohanty, S.; Nayak, S. K. *Polym. Compos.* **2012**, *33*, 22.
17. Kulkarni, M. B.; Mahanawar, P. A. *J. Thermoplast Compos.* **2014**, DOI: 10.1177/0892705713518795.
18. Das, K.; Ray, D.; Adhikary, K.; Bandyopadhyay, N. R.; Mohanty, A. K.; Misra, M. *J. Reinf. Plast. Compos.* **2009**, *29*, 510.
19. Wang, Z.; Lu, Y.; Liu, J.; Dang, Z.; Zhang, L.; Wang, W. *Polym. Adv. Technol.* **2011**, *22*, 2302.
20. Kamal, M.; Sharma, C. S.; Upadhyaya, P.; Verma, V.; Pandey, K. N.; Kumar, V.; Agarwal, D. D. *J. Appl. Polym. Sci.* **2012**, *124*, 2649.
21. Yao, N.; Zhang, P.; Song, L.; Kang, M.; Lu, Z.; Zheng, R. *Appl. Surf. Sci.* **2013**, *279*, 109.
22. Sengupta, S.; Maity, P.; Ray, D.; Mukhopadhyay, A. *J. Appl. Polym. Sci.* **2013**, *130*, 1996.
23. Sengupta, S.; Ray, D.; Mukhopadhyay, A. *ACS Sustainable Chem. Eng.* **2013**, *1*, 574.
24. Sengupta, S.; Pal, K.; Ray, D.; Mukhopadhyay, A. *Compos. B.* **2011**, *42*, 1834.
25. Sengupta, S.; Maity, P.; Ray, D.; Mukhopadhyay, A. *Adv. Mater. Res.* **2012**, *584*, 551.
26. In Book of Standards; ASTM D 790-10; American Society for Testing and Materials: West Conshohocken, PA, Vol. 08.01, **2010**.
27. Chabri, S.; Chatterjee, S.; Pattanayak, S.; Chakraborty, H.; Bhowmik, N.; Sinha, A. *J. Mater. Sci. Technol.* **2013**, *29*, 1085.
28. Vander Merwe, E. M.; Prinsloo, L. C.; Kruger, R. A.; Mathebula, L. C. Presented at World of Coal Ash (WOCA) Conference, Denver, CO, May **2011**. http://www.flyash.info/2011/083-vanderMerwe-2011.pdf.

29. Celik, Ö.; Damci, E.; Pişkin, S. *Indian J. Eng. Mater. Sci.* **2008**, *15*, 433.

30. Lima, D. G.; Soares, V. C. D.; Ribiero, E. B.; Carvalho, D. A.; Cardoso, É. C. V.; Rassi, F. C.; Mundin, K. C.; Rubim, J. C.; Suarez, P. A. Z. *J. Anal. Appl. Pyrolysis* **2004**, *71*, 987.

31. Ray, D.; Sengupta, S.; Sengupta, S. P.; Mohanty, A. K.; Misra, M. *Macromol. Mater. Eng.* **2006**, *291*, 1513.

32. Das, K.; Ray, D.; Banerjee, C.; Bandyopadhyay, N. R.; Misra, M. *J. Appl. Polym. Sci.* **2011**, *119*, 2174.

33. Patnaik, A.; Satpathy, A.; Mahapatra, S. S.; Dash, R. R. *J. Reinf. Plast. Compos.* **2009**, *28*, 1305.

34. Temurijin, J.; Williams, R. P.; Van Riessen, A. *J. Mater. Process. Technol.* **2009**, *209*, 5776.

35. Sarazin-Perrin, F.; Ton That, M. T.; Bureau, M. N.; Renault, J *Polymer* **2005**, *46*, 11624.